


Mechanism of Ultrasound Scission of a Silver–Carbene Coordination Polymer

Joost Rooze,[†] Ramon Groote,^{‡,§} Robert T. M. Jakobs,^{‡,§} Rint P. Sijbesma,^{*,‡,§} Maikel M. van Iersel,^{||} Evgeny V. Rebrov,^{⊥,†} Jaap C. Schouten,^{†,§} and Jos T. F. Keurentjes^{†,||}

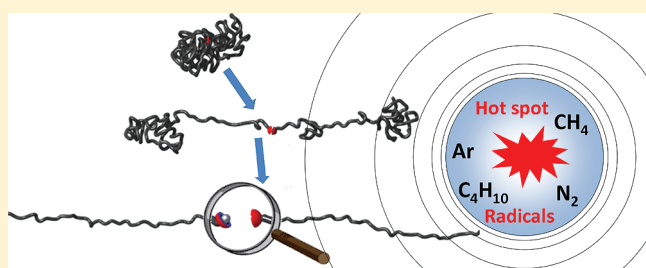
[†]Laboratory of Chemical Reactor Engineering, [‡]Laboratory for Macromolecular and Organic Chemistry, and [§]Institute for Complex Molecular Systems, Eindhoven University of Technology, P.O. Box 513, 5600 MB Eindhoven, The Netherlands

^{||}AkzoNobel Industrial Chemicals, P.O. Box 247, 3800 AE Amersfoort, The Netherlands

[⊥]School of Chemistry and Chemical Engineering, Queen's University Belfast, BT9 5AG, Belfast, United Kingdom

 Supporting Information

ABSTRACT: Scission of a supramolecular polymer–metal complex can be carried out using collapsing cavitation bubbles created by ultrasound. Although the most plausible scission mechanism of the coordinative bonds is through mechanical force, the influence of radicals and high hot-spot temperatures on scission has to be considered. A silver(I)–N-heterocyclic carbene complex was exposed to 20 kHz ultrasound in argon, nitrogen, methane, and isobutane saturated toluene. Scission percentages were almost equal under argon, nitrogen, and methane. Radical production differs by a factor of 10 under these gases, indicating that radical production is not a significant contributor to the scission process. A model to describe the displacement of the bubble wall, strain rates, and temperature in the gas shows that critical strain rates for coil-to-stretch transition, needed for scission, are achieved at reactor temperatures of 298 K, an acoustic pressure of 1.2×10^5 Pa, and an acoustic frequency of 20 kHz. Lower scission percentages were measured under isobutane, which also shows lower strain rates in model simulations. The activation of the polymer–metal complexes in toluene under the influence of ultrasound occurs through mechanical force.



INTRODUCTION

Chemical bonds can be activated by mechanical forces, instead of by using conventional means such as thermal or photochemical activation.^{1,2} The energy landscape of mechanically and thermally activated reactions is sometimes substantially different, resulting in different reaction pathways for each activation method.^{2–5} A handle is required for efficient transduction of (external) mechanical forces onto the chemical bond that needs to be activated. Polymer chains have shown to be very effective for this purpose.^{1,5–11} The use of mechanical forces to carry out chemical transformation within molecules has recently gained interest as it opens the way to the development of mechano-responsive materials (e.g., materials that give a color change upon strain⁶ or self-healing materials). In this respect, it is especially interesting to look at activation of catalytic processes induced by mechanical forces (mechanocatalysis).^{10–12} Recent work has shown the promising prospects of using mechanical forces for activation of latent transition metal complexes,^{11,12} which can subsequently be used as catalysts. Transesterification and metathesis reactions have been successfully performed by subjecting a solution of the polymer mechanocatalyst complexes to ultrasound irradiation in the presence of reactants.^{10,12} Activation of the organometallic complexes is achieved by breakage of the coordination bond between the metal center and the

N-heterocyclic carbene (NHC) ligand. This leads to either an active ruthenium(II)–NHC Grubbs catalyst, widely used as an olefin metathesis catalyst,¹³ or a free NHC, which is an organocatalyst commonly used in, e.g., ring-opening polymerization reactions of cyclic esters^{14–16} and transesterification reactions.^{17,18} The silver(I)–NHC complex is of interest in this study as it has a low critical molecular weight for scission with ultrasound.¹¹ The polymer chains attached to the complex are short, and scission can therefore be measured directly by ¹H NMR spectroscopy. A free NHC is formed in solution when scission of the silver(I)–NHC bond occurs (see Figure 1), which can re-coordinate to a silver(I) ion since the complexed and free NHCs are in a dynamic equilibrium. However, if a source of protons (such as water) is present, the strongly basic NHC is converted to the corresponding imidazolium salt, and reformation of the complex is prevented. The solvent toluene was saturated with water to scavenge the free NHCs during the sonication experiments.

Ultrasound in a liquid can create the forces needed for mechanoscission, by inducing growth of gaseous nuclei, which subsequently collapse.¹⁹ This process is called cavitation, and it

Received: April 23, 2011

Revised: August 7, 2011

Published: August 09, 2011

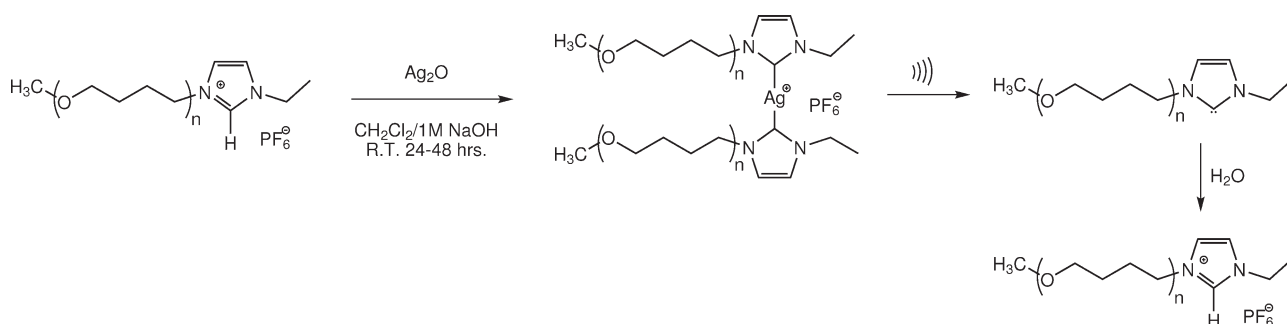


Figure 1. Schematic overview of the synthesis and mechanochemical scission of the silver(I)–NHC polymer catalyst complex by ultrasound and the subsequent reaction of the free NHC with water.

may lead to radical formation,²⁰ high heating and cooling rates,²¹ and polymer scission.²² Radical formation results from the dissociation of gas molecules at the high temperatures and pressures inside the bubble during the collapse due to compression. High temperatures are also reached because the collapse time is shorter than the relevant times for mass and heat transfer. Polymer scission is caused by the high strain rates generated at the bubble wall. The strain rates are in the order of 10^7 s^{-1} .^{9,22,23} The resulting forces are large enough to induce stretching and breaking of a covalent bond in a polymer above a critical molecular weight.^{22,24} There is a strong influence of gas solubility on the efficiency of an ultrasonic scission process as was demonstrated in the work by Price et al. on scission of covalent polymers.²⁵ They found that ultrasonic scission was less efficient under gases with a high solubility.

Here, the relative contributions of mechanical scission, thermal, and radical-induced dissociation mechanisms to ultrasonic scission of a silver(I)–NHC coordination bond are investigated. The bubble internal and interface temperatures and the radical production rate are varied by using different saturation gases (argon, nitrogen, methane, and isobutane) during ultrasound experiments. Both polymer scission and radical production experiments are compared with a model of the radial dynamics of a gas bubble under the influence of an ultrasound field to identify the relevant scission pathways. The scission and radical production experiments are presented first, followed by a qualitative interpretation of the results using the model.

EXPERIMENTAL SECTION

Synthesis of the Polymer–Metal Complex. All solvents used in the synthesis and workup were obtained from BioSolve and of at least AR grade quality and used without further purification, unless otherwise stated. *N*-Ethyl imidazole-terminated ω -methoxy poly(tetrahydrofuran) polymer was synthesized via cationic ring-opening polymerization of 75 mL of tetrahydrofuran (THF) using 100 μL of methyl triflate (purity 98%, Sigma-Aldrich) as initiator,¹¹ and 50 μL of di-*tert*-butyl pyridine (Sigma-Aldrich) was added as a base. The polymerization was carried out under an inert argon atmosphere using Schlenk line techniques. THF was dried and purified by passage over an alumina-packed column prior to use. After 2.5 h, the polymerization was terminated by adding approximately 200 μL (2 mol equiv with respect to the initiator) of *N*-ethyl imidazole (98%, TCI). The polymer was obtained as white powder in good quantity after precipitation of the crude polymer (obtained as a colorless oil) in water (overnight at ambient temperature) and

diethyl ether (overnight at 253 K). Ion exchange to the chloride anion was carried out by stirring the polymer with Dowex exchange resin (1×8 50–100 mesh, Acros) in methanol for 2–3 h. The exchange resin was then removed by filtration, and the methanol was evaporated in vacuo. Subsequent ion exchange of the chloride to the hexafluorophosphate (PF_6^-) anion was carried out by stirring the polymer in the presence of an excess (1.1–1.5 equiv) of ammonium hexafluorophosphate (99.99%, Acros) in methanol for 2–3 h, followed by evaporation of the solvent in vacuo. The polymer was characterized after synthesis and workup by ^1H NMR in acetone- d_6 (Cambridge Isotope Laboratories, Inc.) on a 400 MHz Varian spectrometer to confirm end-group functionalization of the polymer and to determine the number-average molecular weight, M_n . Gel permeation chromatography (GPC) was carried out on a Polymer Laboratories PL-GPC 50 system using DMF/LiBr as eluent. ^1H NMR analysis confirmed end-functionalization with *N*-ethyl imidazole and gave an estimated number-average molecular weight of 7.82 kg mol^{-1} . This value is in good agreement with the results obtained from GPC analysis on this polymer: $M_n = 7.18 \text{ kg mol}^{-1}$ with a narrow polydispersity index (1.11). A typical ^1H NMR spectrum of the polymer is provided as Supporting Information.

Complexation of the *N*-ethyl imidazole-terminated polymer with silver(I) was typically performed by stirring 500 mg of polymer with an excess of silver(I) oxide (99%, Sigma-Aldrich) in 5–10 mL of dichloromethane and 1 mL of 1 M NaOH solution for 24–48 h at ambient temperature. Approximately 5 mg of tetrabutyl ammonium hexafluorophosphate (98%, Acros) was added as the phase transfer catalyst. Workup of the complex was done by separating the dichloromethane/water layers, followed by filtration of the dichloromethane layer over Celite to adsorb small ionic species. The filtrate was dried with magnesium sulfate and filtered. The dichloromethane was subsequently evaporated to obtain the polymer complex in good yields. A typical ^1H NMR spectrum of the complex is provided as Supporting Information to this paper.

Sonication Experiments. A homemade, double-jacketed glass reactor with a volume of 10 mL was used in the sonication experiments. A Sonics and Materials 20 kHz, 0.5 in. diameter titanium alloy ultrasound probe with half wave extension (parts 630-0220 and 630-0410) was operated using a Sonics and Materials VC750 power supply. The temperature in the reactor was maintained with a Lauda E300 cooling bath and measured using a 0.5 mm diameter thermocouple. Isobutane (99.5 vol. %, Linde), methane (99.995 vol. %, Linde), nitrogen (99.999 vol. %, Linde), or argon (99.996 vol. %, Linde) was bubbled at 5 mL min^{-1}

through the experimental solution for at least 30 min prior to and during all experiments. The gas flow rate was controlled using a mass flow controller (Bronkhorst High-Tech B.V., F-201CV).

The polymer–metal complex (15 mg) was dissolved in 5 mL of toluene (AR grade, Biosolve) that was saturated with demineralized water prior to use. The solution was then transferred into the reactor and was allowed to saturate with argon, nitrogen, methane, or isobutane for at least 30 min prior to sonication. During this time, the solution was kept at 283 K. The solution was sonicated for 5 min at 25% of the maximum amplitude (corresponding to an input power into the liquid of 12–17 W, varying per experiment) after gas saturation. The solution temperature inside the reactor increased to 301 ± 4 K during the first minute and was constant afterward. The whole solution was removed from the reactor when the sonication was stopped, and the solvent was evaporated in vacuo. The residual solid was redissolved in ca. 600 μ L of acetone- d_6 to allow determination of the extent of scission by ^1H NMR (see Supporting Information for details on the analysis procedure). The scission percentage is defined as the fraction of the integrated NMR peak of the ligand over that of the initial complex (see Supporting Information).

For radical formation measurements, a volume of 10 mL of the radical scavenger 1,1-diphenyl-2-picryl-hydrazyl (DPPH) with a concentration of $30 \mu\text{mol L}^{-1}$ in toluene (99.8 wt %, Aldrich) was sonicated for 5–30 min after saturation with argon, nitrogen, methane, or isobutane at a temperature of 279–288 K. The power delivered to the liquid was 10–30 W (20–30% of the maximum amplitude). The initial temperature was varied so that the final temperature was 298 ± 3 K after 1 min. DPPH reacts to 2,2-diphenyl-1-picrylhydrazine (DPPH_2) with H radicals, if present.^{26–28} UV spectroscopy (Shimadzu 2501-PC) was used for product analysis. Absorption peaks at 330 and 520 nm were assigned to DPPH and that at 380 nm to DPPH_2 . The 520 nm peak was selected for analysis because it was relatively isolated from the other peaks. Gaussian peak fitting between 440 and 580 nm with a DPPH_2 baseline correction yielded concentration values. The number of experiments was at least 6 for each gas, with 1 to 6 sample points per experiment. Only the measurements obtained in the linear part of DPPH concentration decline were used when calculating the reaction rate.

Bubble Oscillation Model. The bubble oscillation model of van Iersel et al.²⁹ which is based on the model by Yasui³⁰ has been used to describe the displacement of the wall of a spherical gas bubble in a liquid under influence of a pressure field. It also describes thermodynamic properties such as the bubble temperature and pressure. The model consists of a Keller–Miksis variation of the Rayleigh–Plesset equation,³¹ a Hertz–Knudsen–Langmuir description of vapor transport across the bubble–liquid interface,³⁰ coupled with Maxwell–Stefan diffusion equations,³² and an energy balance (see Supporting Information for the equations and pure-component properties; further elaboration on the model and its assumptions is present in the literature²⁹).

The model has been simplified to make it more robust. The ideal gas equation has been used for the description of the gas in the cavity instead of the van der Waals equation because the latter gives singularities in a number of simulations when the pressure approached the maximum theoretical van der Waals pressure. Hot-spot temperature changes by chemical reactions have not been taken into account in this model. The relation $\varepsilon = -2\dot{R}/R$ has been used to calculate the strain rate at the wall of a collapsing bubble,^{9,33} where ε is the strain rate, \dot{R} the bubble wall velocity,

Table 1. Model Parameters

parameter	symbol	value
acoustic pressure	P_a	$1.2 \times 10^5 \text{ N m}^{-2}$
frequency	f	20 kHz
initial pressure	P_0	$1.0 \times 10^5 \text{ N m}^{-2}$
initial temperature	T_0	298 K

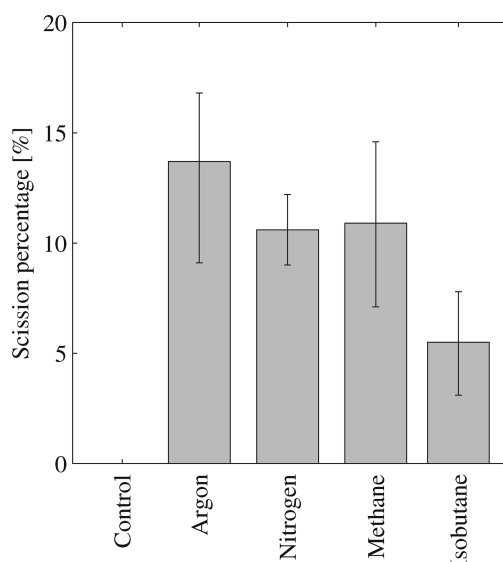


Figure 2. Scission percentage of the silver(I)–NHC complex in toluene at 301 K saturated with argon, nitrogen, methane, and isobutane after 5 min of sonication and a power input of 16, 17, 15, and 12 W, respectively. The percentage of scission is averaged over two or three experiments. The error bars are the minimum and maximum value. No scission is observed in control experiments.

and R the bubble radius. It is expected that the scission percentage scales with the strain rate because the critical strain rate is attained in a larger volume around the collapsing bubble at increasing strain rate near the bubble wall. The silver–NHC complex chains have to be (partially) extended by the strain rates before the polymer complex can undergo mechanical scission.^{9,24,34} The transition of conformation of a polymer chain from a random coil to a stretched state occurs when $\varepsilon \times \lambda_0 \approx 1$,^{24,34} where λ_0 is the relaxation time. Determination of the relaxation times of these polymer–metal complexes based on viscosity measurements has shown that the critical strain rates for coil-to-stretch transition are in the order of 10^6 – 10^7 s^{-1} . (The longest characteristic relaxation time of a polymer chain in dilute solution is calculated according to $\lambda_0 = \eta_0 \times \eta_{\text{solvent}}^{-1} M R_g^{-1} T^{-1}$.³⁵ For covalent poly(tetrahydrofuran) in toluene, the intrinsic viscosity $[\eta]_0 = 5.5 \times 10^{-3} \text{ M}^{0.78} \text{ L g}^{-1}$; the viscosity of toluene $\eta_{\text{solvent}} \approx 10^{-3} \text{ Pa s}$; and $R_g T$ is 2500 J mol^{-1} at room temperature. Substitution of the values results in $\lambda_0 \approx 2.2 \times 10^{-9} \text{ M}^{1.78} \text{ s}$, and a longest characteristic relaxation time of the polymer chain of $\lambda_0 \approx 10^{-7} \text{ s}$ with $M \approx 10 \text{ kg mol}^{-1}$).

The NDSolve function with varying time step in Mathematica (Wolfram Research, version 6.0.3.0) has been used to solve the system of ordinary differential equations and linear equations, using the model settings shown in Table 1. The interface temperature has been used as an indication for the degree of thermal

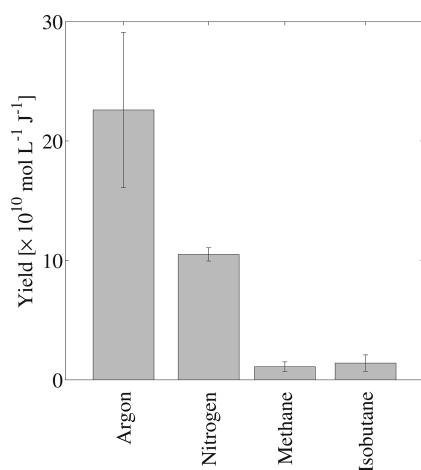


Figure 3. DPPH₂ production per Joule energy input at 298 K in argon, nitrogen, methane, and isobutane saturated toluene. The error bars represent the standard deviation.

scission. The possible effect of droplet injection from a distorted bubble interface³⁷ is not taken into account. Bubble oscillations have been calculated for multiple initial bubble radii from 1 to 50 μm with a step of 1 μm . The results obtained can not directly be related to a bubble in the multibubble field generated in the experiments since the sound field inside the liquid is not expected to be uniform due to distortions and reflections by other bubbles and due to possible break-up of the bubble during the collapse. Interpretation of the results by comparing various gases and liquids yields the most insight. Conclusions have been drawn based on comparisons.

RESULTS AND DISCUSSION

Sonication of Polymer Complex Solutions. The measured scission percentages of the silver(I)–NHC complex in argon, nitrogen, and methane saturated toluene after 5 min of sonication are similar (11–14%, see Figure 2). A slightly lower scission percentage of 6% is observed in an isobutane saturated toluene solution. The thermal background conversion at 283 K in toluene measured without exposure to ultrasound is less than 1%. When the silver(I)–NHC complex in toluene is kept at 383 K for 1 h, 20% scission is observed.

Radical Formation Measurements. The radical formation rate has been measured spectroscopically using the radical scavenger DPPH. Reaction yields are shown in Figure 3. The highest reaction yield of $23 \times 10^{-10} \text{ M J}^{-1}$ is found under argon. An intermediate reaction yield of $11 \times 10^{-10} \text{ M J}^{-1}$ is found under nitrogen, and low reaction yields of 1.1 and $1.4 \times 10^{-10} \text{ M J}^{-1}$, respectively, are found under methane and isobutane (see Figure 3). The measured reaction constants of DPPH conversion under argon ($17\text{--}70 \text{ nmol L}^{-1} \text{ s}^{-1}$) are of the same order of magnitude as those measured by Suslick et al. ($36 \text{ nmol L}^{-1} \text{ s}^{-1}$) under similar conditions.²⁸

There is a different trend in the radical and scission experiments when varying the dissolved gas type. There is only a small difference between the efficacy of the gases in the scission experiments and a large difference in the radical experiments. These results are consistent with previous experimental work on scission with polymers of varying length¹¹ and indicate that

radical production has a negligible influence on the scission process.

Modeling. A model has been used to obtain insight into the possible activation pathways. The bubble radii for argon, nitrogen, and methane saturated toluene are approximately the same during the ultrasound cycle; therefore, only results for argon and isobutane saturated solutions are depicted in Figure 4. The strain rates are larger than 10^7 s^{-1} , which is the estimated strain rate for coil-to-stretch transition of the polymer–metal complexes under all gases except isobutane at small initial radii ($<8 \mu\text{m}$). The strain rate at collapse in the isobutane saturated toluene solution is lower than that of the other gases due to a slower collapse. The collapse is cushioned by a higher number of isobutane molecules inside the bubble in isobutane saturated toluene than in argon saturated toluene. The strain rates averaged over all collapses and all initial bubble radii are between 65 and $75 \times 10^6 \text{ s}^{-1}$ for argon, nitrogen, and methane saturated toluene. It is $9 \times 10^6 \text{ s}^{-1}$ when using isobutane. This trend is similar to that observed in scission experiments, where these three gases have approximately equal scission percentages and isobutane has a lower scission percentage.

A hot spot is formed during the collapse due to compression of the gas. The heat that is released is subsequently transported to the gas–liquid interface and further into the liquid.³⁸ The maximum hot-spot temperatures in the gas vary with the heat capacity of the gases. The calculated temperatures are given as maximum values for each initial radius averaged over all initial radii, with the standard deviation. The hot spot temperature is $580 \pm 50 \text{ K}$ for argon, $560 \pm 40 \text{ K}$ for nitrogen, $520 \pm 30 \text{ K}$ for methane, and $460 \pm 10 \text{ K}$ for isobutane. The larger the initial bubble radius, the lower the bubble vapor content, and the higher the hot-spot temperature. The heat capacity changes with the density and is therefore a factor of 1000 higher in the liquid than in the gas. The maximum liquid interface temperature averaged over all initial bubble radii is $335 \pm 20 \text{ K}$ under argon, nitrogen, and methane and $310 \pm 10 \text{ K}$ under isobutane. The calculated temperatures are lower than those reported in the literature obtained spectroscopically by Didenko et al. for octanol (4300 K) and dodecane (3200 K).³⁹ These solvents have a much lower vapor pressure (3 and 9 Pa, respectively) than toluene (1300 Pa), and therefore much higher hot-spot temperatures are expected. Mišík and Riesz⁴⁰ have reported a hot-spot temperature measured by thermometry of 6300 K. The reason for the discrepancy between these results and the temperatures obtained by Didenko et al. is unknown; possibly the ultrasound conditions are different for both experiments.

The model provides insight into the relations between hot-spot and interface temperature, strain rates and bubble collapse velocity, heat capacity and heat conduction, and gas solubility. The strain rate and the hot-spot temperature vary with the dissolved gas, although a constant scission value is measured experimentally in toluene. The strain rates averaged over multiple collapses and initial bubble radii are similar for argon, nitrogen, and methane. The calculated values of strain rate and hot-spot temperature cannot be considered quantitative since they strongly depend on the conditions upon collapse. The assumptions of the model and the equation of state are not valid anymore at the final stage of bubble collapse. The model results can therefore only be considered in a qualitative way. Thermal dissociation of the silver(I)–NHC bond can not be excluded at the calculated liquid interface temperatures. The radical production experiments can be qualitatively evaluated using results

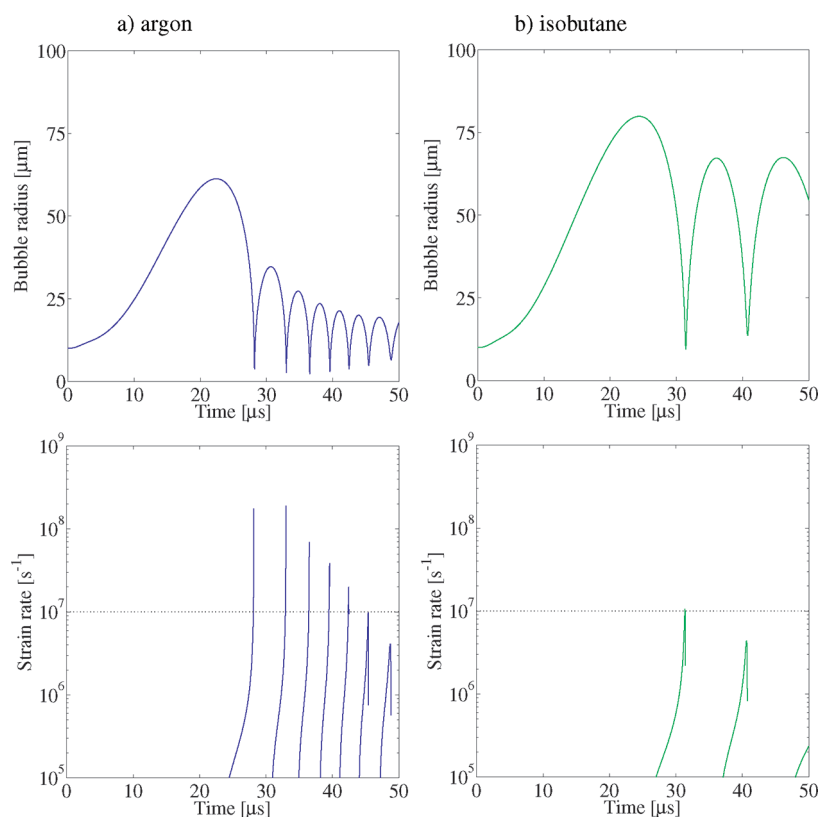


Figure 4. Modeled radial dynamics (top) and strain rate (bottom) for oscillation of a bubble with an initial radius of 10 μm in toluene saturated with (a) argon and (b) isobutane.

from the model. Szwarc reports pyrolysis of toluene at temperatures of 738 K and higher.⁴¹ This temperature is feasible in hot spots during ultrasonic cavitation, although the modeled hot-spot temperatures are lower (the maximum temperature obtained is 690 K for an argon bubble with an initial radius of 46 μm). However, the calculated temperatures are averaged over the entire bubble volume, so the temperatures in the center of the bubble are expected to be higher than the average values. The experimental radical production rate coefficients qualitatively agree with modeled maximum hot-spot temperatures, where the experiments with higher hot-spot temperatures had higher radical production rates than those with lower hot-spot temperatures. The hot-spot interface temperatures are moderate, around 335 K, but may be a cause for thermal scission. However, the complex is not necessarily present at the gas–liquid interface and may therefore experience a lower temperature.

The gas solubility seems to have a strong influence on radial dynamics, strain rates, and temperature maxima, which has been reported before using several observation methods (covalent polymer scission, sonoluminescence, and radical production).^{25,42–44} The gases with a higher solubility showed less intense cavitation effects in these studies. Cushioning of the collapse by mass transport into the bubble may be a cause for these effects.

CONCLUSIONS

Scission of a polymer silver(I)–*N*-heterocyclic carbene complex by ultrasound has been investigated experimentally and theoretically to provide insight into the most likely scission

mechanism. The mechanisms considered include thermal scission, scission by radicals, and mechanical scission by strain imposed on the polymer chain during collapse of the cavitation bubble.

Experimental studies have been performed using argon, nitrogen, methane, and isobutane as saturation gases in toluene. The physical properties of the cavitation bubble have been varied to be able to discern the dominant scission mechanism. Scission after five minutes of sonication varied by a factor of approximately 2, from 6% under isobutane to 11–14% for the other gases. Experiments using DPPH as a radical scavenger showed that the radical production rate varied by an order of magnitude using the various saturation gases. These experimental findings, which are supported by numerical modeling of the cavitation bubble collapse, indicate that the effect of radicals can be excluded as the predominant mechanism for polymer chain scission. Modeling also indicated that solvent temperature increase at the bubble interface is moderate. The numerical simulations have indicated that the critical strain rates required to fulfill the coil-to-stretch can be achieved in the sonication experiments. Therefore mechanical forces in solution arising from the collapse of cavitation bubbles are the most likely cause of scission. This conclusion is in line with the observation of molecular weight dependent scission rates,¹¹ which also indicate a mechanical origin of scission by ultrasound.

It is of interest to implement the findings of this study in future work on mechanocatalysis experiments, such as transesterification reactions or ring-closing metathesis reactions, using the Grubbs polymer catalyst.

■ ASSOCIATED CONTENT

S Supporting Information. Model equations, pure component properties used in the model, determination of the percentage of catalyst scission from ^1H NMR, and nomenclature. This material is available free of charge via the Internet at <http://pubs.acs.org>.

■ AUTHOR INFORMATION

Corresponding Author

*E-mail: r.p.sijbesma@tue.nl.

■ ACKNOWLEDGMENT

The financial support by the Dutch Technology Foundation STW (project number EPC 7391), the Dutch National Research School Combination Catalysis Controlled by Chemical Design (NRSC-Catalysis), and The Netherlands Organisation for Scientific Research (NWO) is gratefully acknowledged. Contributions from Bunova, Intelligent Laser Applications, KWR, and Micronit to STW project EPC 7391 are gratefully acknowledged.

■ REFERENCES

- (1) Beyer, M. K.; Clausen-Schaumann, H. *Chem. Rev.* **2005**, *105*, 2921–2948.
- (2) Ribas-Arino, J.; Shiga, M.; Marx, D. *Angew. Chem., Int. Ed.* **2009**, *48*, 4190–4193.
- (3) Ribas-Arino, J.; Shiga, M.; Marx, D. *Chem.—Eur. J.* **2009**, *15*, 13331–13335.
- (4) Ong, M. T.; Leiding, J.; Tao, H.; Virshup, A. M.; Martínez, T. J. *J. Am. Chem. Soc.* **2009**, *131*, 6377–6379.
- (5) Hickenboth, C. R.; Moore, J. S.; White, S. R.; Sottos, N. R.; Baudry, J.; Wilson, S. R. *Nature* **2007**, *446*, 423–427.
- (6) Davis, D. A.; Hamilton, A.; Yang, J.; Cremer, L. D.; Van Gough, D.; Potisek, S. L.; Ong, M. T.; Braun, P. V.; Martínez, T. J.; White, S. R.; Moore, J. S.; Sottos, N. R. *Nature* **2009**, *459*, 68–72.
- (7) Paulusse, J. M. J. *Ph.D. thesis*, Eindhoven University of Technology, 2006.
- (8) Potisek, S. L.; Davis, D. A.; Sottos, N. R.; White, S. R.; Moore, J. S. *J. Am. Chem. Soc.* **2007**, *129*, 13808–13809.
- (9) Kuipers, M. W.; Iedema, P. D.; Kemmere, M. F.; Keurentjes, J. T. F. *Polymer* **2004**, *45*, 6461–6467.
- (10) Piermattei, A.; Karthikeyan, S.; Sijbesma, R. P. *Nat. Chem.* **2009**, *1*, 133–137.
- (11) Karthikeyan, S.; Potisek, S. L.; Piermattei, A.; Sijbesma, R. P. *J. Am. Chem. Soc.* **2008**, *130*, 14968–14969.
- (12) Tennyson, A. G.; Wiggins, K. M.; Bielawski, C. W. *J. Am. Chem. Soc.* **2010**, *132*, 16631–16636.
- (13) Trnka, T. M.; Grubbs, R. H. *Acc. Chem. Res.* **2001**, *34*, 18–29.
- (14) Sentman, A. C.; Csikony, S.; Waymouth, R. M.; Hedrick, J. L. *J. Org. Chem.* **2005**, *70*, 2391–2393.
- (15) Kamber, N. E.; Jeong, W.; Gonzalez, S.; Hedrick, J. L.; Waymouth, R. M. *Macromolecules* **2009**, *42*, 1634–1639.
- (16) Marion, N.; Díez-González, S.; Nolan, S. *Angew. Chem., Int. Ed.* **2007**, *46*, 2988–3000.
- (17) Grasa, G. A.; Kissling, R. M.; Nolan, S. P. *Org. Lett.* **2002**, *4*, 3583–3586.
- (18) Singh, R.; Kissling, R. M.; Letellier, M.-A.; Nolan, S. P. *J. Org. Chem.* **2004**, *69*, 209–212.
- (19) Leighton, T. G. *The acoustic bubble*; Academic Press: London, 1994.
- (20) Makino, K.; Mossoba, M. M.; Riesz, P. *J. Phys. Chem.* **1983**, *87*, 1369–1377.
- (21) Suslick, K. S.; Price, G. J. *Annu. Rev. Mater. Sci.* **1999**, *29*, 295–326.
- (22) Basedow, A. M.; Ebert, K. H. *Ultrasonic Degradation of Polymers in Solution*; Springer-Verlag: Berlin, 1977.
- (23) Weissler, A. *J. Appl. Phys.* **1950**, *21*, 171–173.
- (24) Odell, J. A.; Keller, A.; Muller, A. J. *Colloid Polym. Sci.* **1992**, *270*, 307–324.
- (25) Price, G. J.; Smith, P. F. *Polymer* **1993**, *34*, 4111–4117.
- (26) Sehgal, C.; Yu, T. J.; Sutherland, R. G.; Verrall, R. E. *J. Phys. Chem.* **1982**, *86*, 2982–2986.
- (27) Bawn, C. E. H.; Mellish, S. F. *Trans. Faraday Soc.* **1951**, *47*, 1216–1227.
- (28) Suslick, K. S.; Gawienowski, J. J.; Schubert, P. F.; Wang, H. H. *Ultrasonics* **1984**, *22*, 33–36.
- (29) van Iersel, M. M.; Cornel, J.; Benes, N. E.; Keurentjes, J. T. F. *J. Chem. Phys.* **2007**, *126*, 064508.
- (30) Yasui, K. *Phys. Rev. E* **1997**, *56*, 6750–6760.
- (31) Keller, J. B.; Miksis, M. J. *Acoust. Soc. Am.* **1980**, *68*, 628–633.
- (32) Wesselingh, J. A.; Krishna, R. *Mass transfer in multicomponent mixtures*; Delft University Press: Delft, 2000.
- (33) Agarwal, U. S. *e-Polym.* **2002**, *14*, 1–15.
- (34) Nguyen, T.; Kausch, H.-H. Mechanochemical degradation in transient elongational flow. In *Macromolecules: Synthesis, Order and Advanced Properties*; Springer: Berlin/Heidelberg, 1992; Vol. 100, pp 73–182.
- (35) Larson, R. G. *Constitutive Equation for polymer melts and solutions*; Butterworths: New York, 1988.
- (36) Evans, J. M.; Huglin, M. B. *Die Makromol. Chem.* **1969**, *127*, 141–152.
- (37) Suslick, K. S.; McNamara, W. B., III; Didenko, Y. In *Sonochemistry and sonoluminescence*; Crum, L. A., Mason, T. J., Reisse, J. L., Suslick, K. S., Eds.; Kluwer Academic Publishers: Dordrecht, The Netherlands, 1999; Vol. 524, Chapter Hot spot conditions during multi-bubble cavitation, pp 191–204.
- (38) Suslick, K. S.; Hammerton, D. A.; Cline, R. E. *J. Am. Chem. Soc.* **1986**, *108*, 5641–5642.
- (39) Didenko, Y. T.; McNamara, W. B., III; Suslick, K. S. *Phys. Rev. Lett.* **2000**, *84*, 777–780.
- (40) Mišík, V.; Riesz, P. *Ultrason. Sonochem.* **1996**, *3*, S173–S186.
- (41) Szwarc, M. *J. Chem. Phys.* **1948**, *16*, 128–136.
- (42) Okitsu, K.; Suzuki, T.; Takenaka, N.; Bandow, H.; Nishimura, R.; Maeda, Y. *J. Phys. Chem. B* **2006**, *110*, 20081–20084.
- (43) Wall, M.; Ashokkumar, M.; Tronson, R.; Grieser, F. *Ultrason. Sonochem.* **1999**, *6*, 7–14.
- (44) Brotchie, A.; Statham, T.; Zhou, M.; Dharmarathne, L.; Grieser, F.; Ashokkumar, M. *Langmuir* **2010**, *26*, 12690–12695.